Brain Structure and Function (2020) 225:751–761
https://doi.org/10.1007/s00429-020-02033-6

ORIGINAL ARTICLE

Rostral intralaminar thalamic deep brain stimulation ameliorates memory deficits and dendritic regression in β-amyloid-infused rats

Sheng-Tzung Tsai[1,2] · Shin-Yuan Chen[1,2] · Shinn-Zong Lin[1] · Guo-Fang Tseng[3]

Received: 11 July 2019 / Accepted: 22 January 2020 / Published online: 8 February 2020
© Springer-Verlag GmbH Germany, part of Springer Nature 2020

Abstract

Rostral intralaminar thalamic deep brain stimulation (ILN-DBS) has been shown to enhance attention and cognition through neuronal activation and brain plasticity. We examined whether rostral ILN-DBS can also attenuate memory deficits and impaired synaptic plasticity and protect glutamatergic transmission in the rat intraventricular β-amyloid (Aβ) infusion model of Alzheimer's disease (AD). Spatial memory was tested in the Morris water maze (MWM), while structural synaptic plasticity and glutamatergic transmission strength were estimated by measuring dendritic spine densities in dye-injected neurons and tissue expression levels of postsynaptic density protein 95 (PSD-95) in medial prefrontal cortex (mPFC) and hippocampus. All these assessments were compared among the naïve control rats, AD rats, and AD rats with ILN-DBS. We found that a single rostral ILN-DBS treatment significantly improved MWM performance and reversed PSD-95 expression reductions in the mPFC and hippocampal region of Aβ-infused rats. In addition, ILN-DBS preserved dendritic spine densities on mPFC and hippocampal pyramidal neurons. In fact, MWM performance, PSD-95 expression levels, and dendritic spine densities did not differ between naïve control and rostral ILN-DBS treatment groups, indicating near complete amelioration of Aβ-induced spatial memory impairments and dendritic regression. These findings suggest that the ILN is critical for modulating glutamatergic transmission, neural plasticity, and spatial memory functions through widespread effects on distributed brain regions. Further, these findings provide a rationale for examining the therapeutic efficacy of ILN-DBS in AD patients.

Keywords Cortical plasticity · Thalamus · Deep brain stimulation · Alzheimer's disease

Introduction

Alzheimer's disease (AD) is the most common neurodegenerative disorder throughout the world. At the functional level, AD is characterized by gradual and largely irreversible declines in memory and cognition. At the molecular and neuronal levels, AD is associated with β-amyloid (Aβ) deposition, neuronal death, and circuit disruption in brain regions implicated in memory and higher cognition, including the hippocampus, basal forebrain, and cerebral cortex. Currently, the most widely used treatments for AD are cholinesterase inhibitors, which presumably improve cognitive function by increasing acetylcholine transmission between the basal forebrain and cerebral cortex (Záborszky et al. 2018). However, degeneration of cholinergic circuits is among the earliest pathogenic events in AD; thus, cholinesterase inhibitors usually demonstrate minimal efficacy in the later stages of the disease and are effective only over a limited time window (Scarpini et al. 2003).

Deep brain stimulation (DBS) is a potential alternative with demonstrated clinical efficacy and safety against movement disorders and neuropsychiatric disorders refractory to conventional drug treatments. The therapeutic effects of DBS are believed to result in part from direct activation or inhibition of specific intracerebral targets, but DBS may also influence entire neural circuits spanning widespread brain regions, and has therefore been described as a circuit neuromodulator (Herrington et al. 2016). The rostral part of the intralaminar thalamic nucleus (ILN) has been suggested

✉ Guo-Fang Tseng
guofang@mail.tcu.edu.tw

1 Department of Neurosurgery, Hualien Tzu Chi Hospital, Buddhist Tzu Chi Medical Foundation/Tzu Chi University, Hualien, Taiwan

2 Institute of Medical Sciences, Tzu Chi University, Hualien, Taiwan

3 Department of Anatomy, College of Medicine, Tzu-Chi University, No. 701, Section 3, Jhongyang Road, Hualien 970, Taiwan

as a key hub for cognitive function in humans and animals (Gold and Squire 2006; Mair and Hembrook 2008; Mair et al. 2011) through connections with the hippocampus and medial prefrontal cortex (mPFC) (Van der Werf et al. 2002; Saalmann 2014). Shirvalkar et al. (2006) reported that a single train of high frequency DBS over the ILN enhanced object recognition memory in healthy rodents. Moreover, this effect was associated with neuronal activation in limbic and neocortical structures essential for memory performance, including the dentate gyrus and hippocampus, as revealed by upregulation of the immediate-early genes c-fos and zif268 (Shirvalkar et al. 2006).

A number of studies have also demonstrated that DBS of the fornix can improve memory impairments in animal models (Hamani et al. 2011; Hescham et al. 2013a, 2016, 2017; Leplus et al. 2019). However, DBS of the fornix has thus far shown only limited efficacy for improving cognitive dysfunction in AD patients (Leoutsakos et al. 2018). Alternatively, the effects of ILN-DBS on AD-associated cognitive deficits have not been studied extensively despite demonstrations of critical ILN functions in cognition functions, including memory, attention, and reward-based learning. To examine whether rostral ILN-DBS can ameliorate AD-associated cognitive deficits and the underlying synaptoplastic abnormalities (Malm et al. 2006), we compared spatial memory performance and measured markers of glutamatergic transmission in the mPFC and hippocampus of rats subjected to intraventricular Aβ infusion with or without subsequent ILN-DBS. This model has been shown to mimic the neuropathological deposition of Aβ protein in AD and to produce phenotypes comparable to sporadic AD (Nitta et al. 1994; Malm et al. 2006; Srivareerat et al. 2009).

Materials and methods

The study was approved by the Animal Care and Use Committee of the Tzu-Chi University and adhered to all relevant institutional and national guidelines for animal welfare. Male Wistar rats (250–350 g body weight) were individually housed under a 12-h light/12-h dark cycle (lights were switched on at 7:00 am) with food and water ad libitum before and during the study period.

β-amyloid protein infusion and ILN-DBS

Rats were assigned to the following groups: (1) naïve controls (control), (2) intraventricular Aβ infusion (AD), and (3) Aβ infusion plus ILN-DBS electrode implantation and stimulation (AD + DBS). These three study groups were used for all the tests performed in this investigation. One additional study group received Aβ infusion plus electrode implantation without stimulation (AD + sham) and was used for the Morris water maze (MWM) test only. AD-simulated rats were implanted with osmotic minipumps (Model: 2002; reservoir volume: 200 µl and 0.5 µl/h infusion rate, Alzet, Cupertino, CA) and skull cannulae for intraventricular delivery of Aβ lasting for 14 days. Briefly, Aβ1–40 and Aβ1–42 peptides (ANASPECT, San Jose, CA) were dissolved in 64.9% sterile distilled water plus 35% acetonitrile and 0.1% trifluoroacetate to prevent Aβ peptide aggregation. Before implantation, minipumps were filled with a 1:1 mixture of Aβ1–40 and Aβ1–42 (priming) and submerged in isotonic saline solution overnight at 37 °C. Immediately prior to minipump and cannula implantation, rats were anesthetized by intraperitoneally injecting them with ketamine and xylazine (8 mg ketamine and 1 mg xylazine/100 g body weight) and mounted on a stereotaxic frame (David Kopf Instruments, Tujunga, CA). An incision was made to expose the skull around the bregma. First, three stainless steel screws were secured halfway into the skull for fixation of the minipump needle cap over the left lateral ventricle and brain stimulation electrode over the right ILN for both AD + sham group and AD + DBS group. In the group receiving only intraventricular Aβ infusion (AD group), one small hole was drilled for needle insertion, whereas two holes were drilled in rats receiving both intraventricular β-amyloid protein and ILN-DBS, one each for the minipump needle and stimulation electrode (comprising twisted stainless steel wires with bare diameter 0.125 mm) (MS303/3-B/SPC; Plastics One, Roanoke, VA). The minipump needle tip was inserted into the left ventricle (AP: − 0.3 mm; ML 2.5 mm; DV: − 4.0 mm, according to Paxinos and Watson (1998) to allow Aβ protein infusion, and the tip of the electrode was inserted into the central lateral nucleus of the right thalamus (AP: − 2.8 mm; ML 1.25 mm; DV − 5.5 mm to bregma) (Fig. 1a). The heads of the minipump needle and electrode were secured with dental cement to the three pre-installed screws, and the wound was closed with nylon sutures. Animals were allowed to recover for 9 days during minipump infusion. Rats in infusion groups received 300 pmol/day of 1:1 Aβ1–40:Aβ1–42 for 2 weeks.

Deep brain stimulation protocol

The rats receiving DBS electrode implantation were treated with a single ILN-DBS stimulation of 30 min immediately before the first MWM training session as described below (Fig. 1b). The stimulating electrode array was connected to a digital bipolar stimulator (Isolated Pulse Stimulator, A-M systems, Sequim, WA) via a spring-shielded stimulating cable (Plastics One, Roanoke, VA) to deliver stimuli of 0.5 mA amplitude and 60 µs duration at 100 Hz for 30 min. In previous studies, constant current of 100–300 µA was used to approximate the response in humans according to generated charge density per phase (Stone et al. 2011).

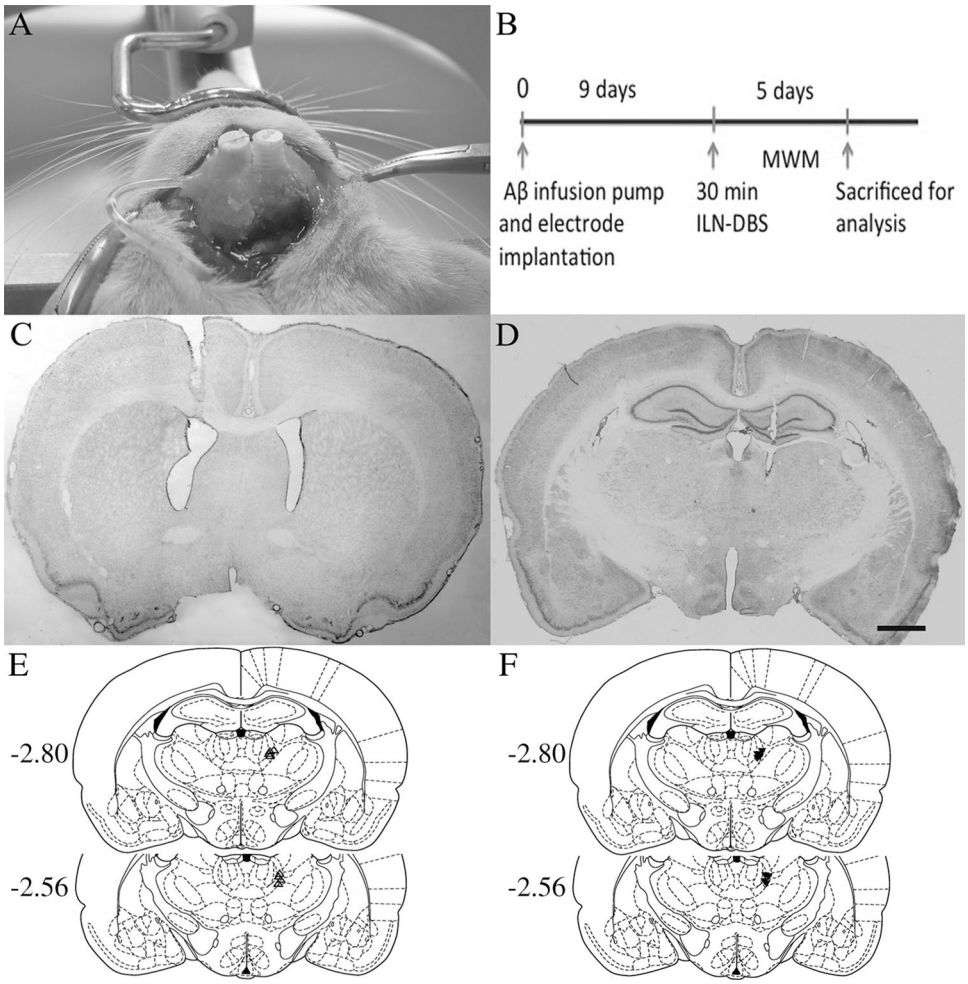

Fig. 1 Animal preparations and protocols for intraventricular infusion of amyloid-beta (AD) and deep brain stimulation of the intralaminar thalamic nucleus (ILN-DBS). **a** Both the DBS electrode and the Alzet osmotic minipump for amyloid-beta infusion were fixed to the skull with dental cement. **b** Schematic diagram illustrating the experimental protocols adopted in the present study. A single train of ILN-DBS was delivered on the first day of Morris water maze training. **c** Nissl staining of coronal brain sections for histological confirmation of minipump needle placement in the left ventricle following experiments. **d** Histological confirmation of DBS electrode placement in the right ILN (arrow). Scale bar = 1 mm. **e** Schematic representation of coronal sections at two rostral–caudal planes showing implantation tip sites of electrodes in AD + sham group. **f** Schematic representation of coronal sections at two rostral–caudal planes showing implantation tip sites of electrodes in AD + DBS group. The numbers on the left indicate locations and coordinates posterior from the bregma

However, we applied 0.5 mA (500 μA) based on recent rodent DBS studies on learning and memory (Shirvalkar et al. 2006; Hamani et al. 2011; Hescham et al. 2013b).

MWM testing

We first examined how AD pathology influenced spatial memory performance in our rat AD model and tested whether clinically relevant DBS stimulation over the ILN could ameliorate cognitive deficits. In the first experiment, 8 naïve control (control) rats, 12 intraventricular Aβ infusion rats (AD), 8 intraventricular Aβ infusion plus sham stimulation (AD + sham) and 9 intraventricular Aβ infusion plus ILN-DBS (AD + DBS) rats were subjected to five consecutive days of MWM training to assess differences in spatial learning capacity (protocol described below). The MWM is widely used to evaluate spatial learning and memory, which requires intact functions of the hippocampus and mPFC (Cholvin et al. 2016). Detailed procedures are described in previous studies (Vorhees and Williams 2006; Tsai et al. 2016).

Briefly, it was conducted in a circular tank with a transparent plastic platform submerged 3 cm below the surface of the water at the center of the target quadrant. In each training session, four consecutive trials starting at the drop-off point of each quadrant of the tank were selected randomly. Animals were allowed to stay on the platform for 15 s after locating it. If they failed to find it within 90 s, rats were gently guided to the platform and remained for 15 s. The time required to find the platform was recorded, analyzed and defined as escape latency. Another probe trial was conducted after day 5 MWM to record the percentages of time they spent in each quadrant of the water maze.

Confirmation of DBS electrode position

To verify the position of the electrode tip, coronal brain sections covering the electrode track were Nissl stained and examined under a microscope. Only rats with verified electrode placement were included in the analyses (Fig. 1c, d). Data from two rats were excluded because of deviation of the electrode position. In addition, sections were immunostained with a rabbit polyclonal antibodies against

Aβ1–42 (ab10148, Abcam Inc., MA) to verify infiltration into brain parenchyma. Staining was conducted according to a previous report (Fig. 2) (Nitta et al. 1994).

Measures of dendritic spine structure

Four control, six AD, and four AD + DBS group rats were subjected to another MWM training and memory session, killed, and examined for structural changes to dendritic arbors and spines in the mPFC and hippocampus by intracellular injection of Lucifer yellow (LY; Sigma, St. Louis, MO) and subsequent immunostaining. Briefly, rats were deeply anesthetized with chloral hydrate (0.9 mg/100 g body weight) and perfused with a fixative containing 2% paraformaldehyde in 0.1 M phosphate buffer (PB, pH 7.3) at room temperature for 30 min. Immediately following perfusion, the whole brain was carefully removed and sectioned with a vibratome into 400-um thick coronal slices including the mPFC and hippocampus. Brain slices were first treated with 0.1 M PB containing 10^{-7} M 4′,6-diamidino-2-phenylindole (DAPI, Sigma) for 30 min to stain cell nuclei blue under the same filter set used for visualizing LY. This enabled us to select individual neurons from specific cortical layers for dye injection. Each slice was then placed in a dish on the stage of a fixed-stage epifluorescence microscope (Olympus BX51) and covered with a thin layer of 0.1 M PB. An intracellular micropipette filled with 4% LY in water was mounted on a three-axial hydraulic micromanipulator (Narishige, Tokyo, Japan) under an objective lens (×20) with long working distance to facilitate the selection of layer III and layer V pyramidal neurons of the mPFC and hippocampal CA pyramidal neurons for dye injection. An intracellular amplifier (Axoclamp-IIB) was used to generate constant negative current for injecting LY until all terminal dendrites fluoresced brightly yellow. Approximately, four to six well-separated neurons could be injected in each slice. The slice was then removed, rinsed in 0.1 M PB, and post-fixed in 0.1 M PB/4% paraformaldehyde for 3 days.

To preserve the intracellular fluorescence and facilitate visualization of dendrites and spines, injected slices were immunostained using an LY antibody. Briefly, the injected slices were rinsed thoroughly in 0.1 M PB, cryoprotected, and carefully sectioned into 50 um serial sections using a sliding microtome. These thin sections were preincubated with 1% H_2O_2 in PB for 30–60 min to block endogenous peroxidase activity, rinsed three times in phosphate-buffered saline (PBS), and incubated for an hour in PBS containing 2% bovine serum albumin plus 1% Triton X-100 for blocking and permeabilization, respectively. Sections were then incubated for 18 h at 4 °C in PBS containing biotinylated rabbit anti-LY (1:200; Molecular Probes, Eugene, OR). Following subsequent rinses in PBS, sections were incubated with standard avidin–biotin horseradish peroxidase reagent (Vector, Burlingame, CA) for 3 h at room temperature. Sections were then reacted at room temperature with a solution containing 0.05% 3,3′-diaminobenzidine tetrahydrochloride (DAB; Sigma) and 0.01% H_2O_2 in 0.05 M Tris buffer. Reacted sections were mounted onto slides for microscopic analysis as described in "Data and statistical analysis" (below).

Western blotting of postsynaptic density protein 95 (PSD-95)

Five control, five AD, and five AD + DBS group rats were subjected to a second MWM training session as described and then killed for western blotting analysis of the glutamatergic postsynaptic marker PSD-95 (Furuyashiki et al. 1999) in the mPFC and hippocampal region. Briefly, the brain regions of interest were rapidly dissected and homogenized immediately at 4 °C in 25 mM 4-(2-hydroxyethyl)-1-piperazineethanesulfonic acid (pH 7.4) containing 0.3 M sucrose, protease inhibitor cocktail, 50 mM sodium vanadate (to inhibit phosphatases), and 0.1 M ethylenediaminetetraacetic acid. Following centrifugation at 600 × 3*g* for 15 min to remove unbroken cells and nuclei, the post-nuclear supernatant was centrifuged at 21,000×*g* to obtain the post-mitochondrial supernatant fraction. Total protein concentration in this fraction was determined using a Bio-Rad assay (Hercules, CA). Next, 20 µg total protein per gel lane was

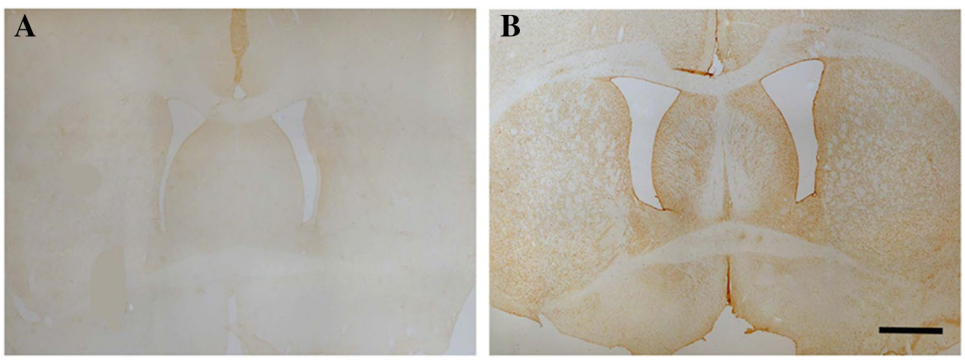

Fig. 2 Immunoreactivity for amyloid-β is increased in coronal sections from rats intraventricularly infused with amyloid-β (**b**) compared with rats without amyloid-β infusion (**a**). Scale bar = 1 mm

separated on 15% acrylamide gels containing sodium dodecyl sulfate and transferred onto polyvinylidene difluoride membranes. Membranes were probed for PSD-95 using mouse anti-PSD-95 (1:1000, Chemicon, Temecula, CA) in 10 mM Tris (pH 7.4) containing 150 mM NaCl and 5% skim milk. A monoclonal antibody to GAPDH (Chemicon) was used as the gel loading control. A similar dilution of the same anti-PSD-95 antibody was used previously to detect PSD-95 in rat brain (Ansari et al. 2008). Protein expression levels were estimated by densitometry. This expression measurement protocol was tested for linearity by varying the amount of protein loaded in different lanes and the exposure time was varied from 10 s to 1 min (or longer if necessary) in 10-s steps. An exposure time of approximately 1 min yielded linear changes in band intensity. Relative optical densities (RODs) of the target band were quantified using a densitometer (ImagePro Plus; Media Cybernetics, Silver Spring, MD) and are presented relative to the ROD of GAPDH for that lane.

Data and statistical analysis

Escape latencies in the MWM training (spatial memory acquisition) phase were compared by two-way repeated measures analysis of variance (ANOVA) with Tukey's post hoc analysis for pairwise multiple comparisons. Fractional search times in the probe test were compared by two-tailed independent samples *t* test and the null hypothesis was a proportion of time in the target zone ≤ 25% (chance or below). All statistical tests were conducted using SPSS 14.0 (SPSS, Chicago, Illinois) and a $p < 0.05$ was considered significant.

For morphometric analyses of pyramidal neuron dendritic arbors from the three treatment groups (20 cells from naïve rats, 30 from Aβ-infused rats, and 20 from Aβ-infused plus ILN-DBS group rats), individual micrographs were reconstructed in three dimensions (3D) using Neurolucida (MicroBrightField, Williston, VT). Spine densities (measurement details below) were compared among groups by one-way ANOVA followed by Newman–Keuls test for pairwise multiple comparisons.

Dendritic spine density is associated with synaptic plasticity (Chen et al. 2013), so we analyzed dendritic spine density from four to six representative pyramidal neurons from layer III and layer V mPFC and from hippocampal CA in each group. Dendrites were selected according to previously established criteria (Chen et al. 2009a). Proximal and distal basal dendrites of layer III pyramidal neurons were defined as the segments 25–50 um and 75–100 um from the soma, respectively, while the proximal and distal basal dendrites of the relatively larger layer V pyramidal neurons were sampled over 50–100 um and 100–150 um from the soma, respectively. The first or second dendritic branch from the apical trunk was designated as the proximal apical dendrite, and the terminal dendritic branch after the last visible branch point of layer III and V pyramidal neurons (usually overlying the junction of cortical layers I and II) was defined as the distal apical dendrite (Fig. 3). For hippocampal pyramidal neurons, spine density was determined from the most lateral tertiary dendrite on the apical tree and the most lateral secondary dendrite on the basal tree. These dendrites were always located within the stratum lacunosum moleculare and the stratum oriens of Ammon's horn, respectively. The representative segments were visualized and analyzed under a 100 × oil immersion objective for manual determination of dendritic spine density (expressed as number per 10 ìm of dendrite length).

Results

Brain deposition of Aβ is a pathological hallmark of AD, and Aβ accumulation has been shown to damage neurons and disrupt transmission in vulnerable regions such as the hippocampus, mPFC, and cholinergic basal forebrain (Ovsepian et al. 2016). To examine the effects of Aβ accumulation on cognitive performance and potential amelioration by ILN-DNS in rats, we compared MWM performance among control rats, AD rats, AD + sham, and AD + DBS. All four groups demonstrated similar performance on the first day of MWM training, but two-way repeated measures ANOVA revealed significant main effects of group ($F_{3, 31} = 4.51$, $p = 0.01$) and training day ($F_{4, 124} = 107.23$, $p < 0.001$). There was no group × day interaction ($F_{4, 124} = 1.1$, $p = 0.366$) on escape latency over the training period. Moreover, post hoc analysis revealed significantly longer average escape latency in the AD and AD + sham groups compared to control ($p < 0.05$). Rostral ILN-DBS on the first day of MWM significantly reversed this spatial learning deficit as evidenced by significantly shorter escape latency compared to the AD + sham and AD groups ($p < 0.05$) (Fig. 4). Further, the probe test conducted on day 5 revealed parallel effects on spatial memory, with control and AD + DBS groups demonstrating significantly longer swim times in the target quadrant compared to the AD + sham group. Alternatively, there were no group differences in swimming speed. Thus, Aβ-induced spatial learning and memory deficits were rescued by a single ILN-DBS treatment.

Since dendritic spine densities of neurons and synaptic plasticity correlated closely with cognitive performance and CNS disease underlying pathology (Schubert et al. 2007; Luebke et al. 2010), we hypothesized that those densities of dendritic spine of pyramidal neurons over mPFC and hippocampus where rostral ILN connects and were integrated within cognitive circuits would have positive association with learning status in different groups. Therefore, additional normal, Aβ infusion only, and Aβ infusion with ILN-DBS

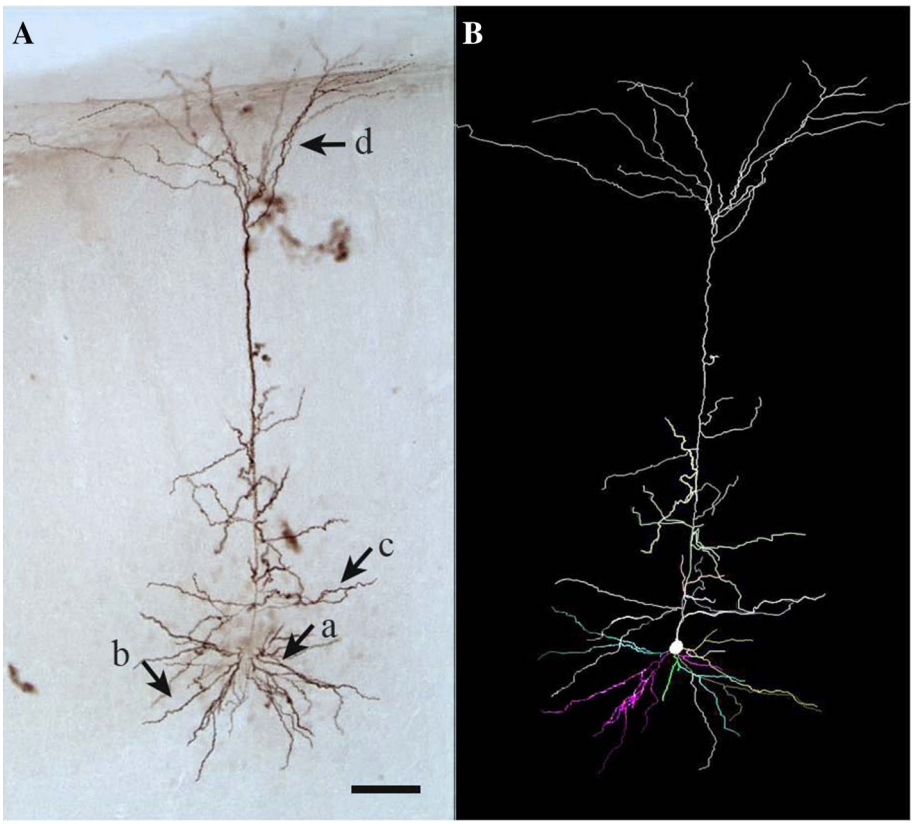

Fig. 3 Intracellular Lucifer yellow injection method for morphometric analysis of medial prefrontal cortex (mPFC) and hippocampal CA pyramidal neurons. **a** Representative layer III mPFC pyramidal neuron from a rat receiving Aβ infusion plus ILN-DBS. a and b proximal and distal basal dendrites, c and d proximal and distal apical dendrites; Scale bar = 70 µm. **b** The dendritic arbors visualized using Neurolucida

rats were subjected to the task of MWM. Immediately after task completion, rats were killed and subjected to intracellular dye injection, allowing us to identify the differences in spine densities on individual neurons. The results showed again that rats treated with Aβ infusion supplemented with rostral ILN-DBS learned as well as control rats, and both groups demonstrated better and faster spatial memory acquisition than rats treated with Aβ infusion alone (Fig. 5a). The behavioral difference was accompanied by variation of dendritic spine densities among the three groups. Rats with intraventricular Aβ infusion demonstrated significantly lower (approximately 50%) spine densities on pyramidal neurons in CA than normal rats, and the spine densities in rats with intraventricular Aβ infusion increased to an extent near to those in control rats after ILN-DBS (Fig. 5b, $p < 0.0001$). In the mPFC, both layer III and layer V pyramidal neurons of the AD rats had remarkably fewer (approximately 36%) densities of dendritic spines than those observed for the naïve control rats (Fig. 6, $p < 0.0001$). Paralleling the findings for dendritic spine densities in CA, the decreased spine densities of mPFC due to Aβ infusion showed a significant restoration after ILN-DBS, to levels similar to the controls ($p < 0.0001$).

To investigate whether the dynamic change of dendritic spine densities represent functional regulation of quantities of excitatory synapses, we performed western blotting and measured the amount of PSD-95, a protein known to associate with glutamatergic excitatory postsynaptic densities and regulate synaptic activity and structural plasticity, in the studied area. Following Aβ infusion, the levels of PSD-95 in the hippocampus and mPF dropped by 50% and 52%, respectively, compared with that of the control rats. In accordance to its effectiveness on dendritic spine densities, rostral ILN-DBS reversed the reductions in PSD-95 in both hippocampus and mPF cortex (Fig. 7, $p < 0.01$).

Discussion

Our key findings are that rats with intraventricular Aβ infusion toxicity showed consistent spatial memory deficit and impaired synaptic plasticity including decreased dendritic spine densities and reduced excitatory synaptic markers. To test a clinically relevant method of reversing cognitive deficit from AD pathology, we used rostral ILN-DBS, and it effectively restored spatial memory performance in the MWM. This improvement was accompanied by increased density of dendritic spines on the dendritic arbors of hippocampal CA pyramidal neurons and medial prefrontal layer III and V pyramidal neurons. These changes in structural plasticity occurred over all the segments of the basal and apical dendrites. Western blotting analysis further confirmed that the fluctuation in numbers of dendritic spines among the three

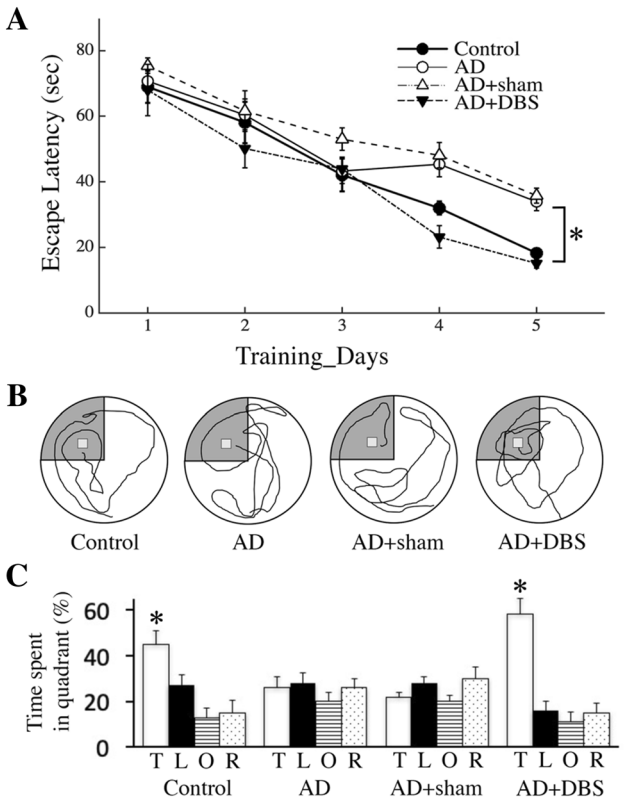

Fig. 4 A single train of rostral ILN-DBS improved the spatial memory acquisition of rats treated with amyloid-β infusion. **a** Plot of the escape latency of the four groups of rats, naïve control rats, AD, AD + sham, and AD + DBS, for 5 consecutive days of MWM assessment. Spatial learning was significantly impaired by Aβ infusion alone and rescued by an ILN-DBS application. $*p < 0.05$, Aβ + ILN-DBS and naïve control vs. AD + sham and AD group. **b**, **c** Representative swim paths during the probe test of spatial memory on day 5. The Aβ + ILN-DBS and naïve control groups spent a significantly higher percentage of the swim time in the target quadrant compared to the AD group (*T* target quadrant, *L*, left quadrant, *O* opposite quadrant, *R* right quadrant); $*p < 0.05$; Error bars show SEM

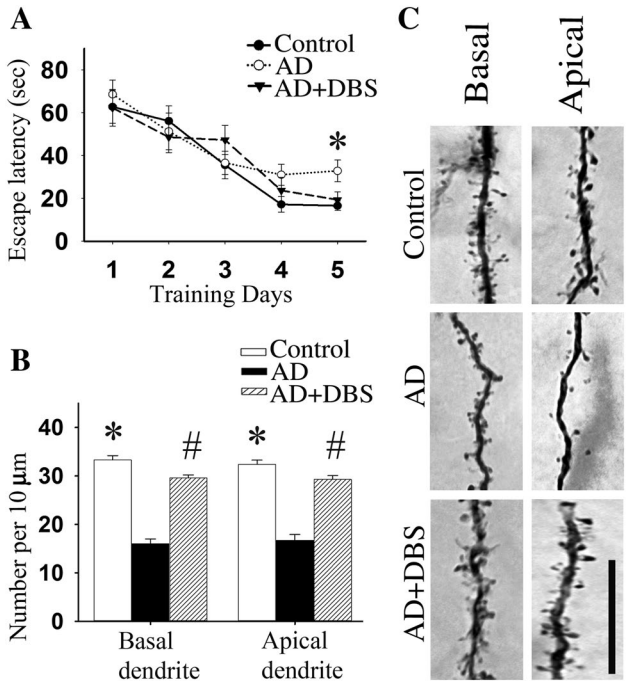

Fig. 5 ILN-DBS reversed Aβ-induced spatial learning and memory deficits and Aβ-induced reduction in hippocampal CA pyramidal neuron spine density. **a** Plot of the escape latencies for AD + DBS, AD alone, and control group rats over the 5 days of MWM training. Escape latencies were significantly shorter in the AD + DBS group compared to the AD group. **b**, **c** Plots of dendritic spine densities and representative images of CA pyramidal neuron apical and basal dendrites. $*p < 0.05$, control vs. AD group. $^{\#}p < 0.05$. AD group vs. AD + DBS group. Scale bar = 10 µm. Error bars represent SEM

groups could be attributed to the regulation of excitatory synaptic protein expression. These data reaffirm previous findings and suggest that rostral ILN-DBS could modulate central neuronal circuits, leading to enhanced excitatory synaptic connectivity in pyramidal neurons of the hippocampal CA and the mPFC (Shirvalkar et al. 2006; Mair and Hembrook 2008). Enhancing the excitability of these neurons may lead to more robust outputs to influence downstream circuits. This is consistent with previous in vivo and clinical studies indicating that ILN-DBS improved cognition (Shirvalkar et al. 2006; Schiff et al. 2007), and it supports the potential use of ILN-DBS-induced enhancement of the attention and frontal arousal circuit in treating patients with cognitive impairment.

ILN-DBS may modulate cerebral cortical and hippocampal circuits through connections from rostral ILN (Van der Werf et al. 2002). Our results echoed a study showing that modulating neural activity of ILN might facilitate working memory task of rats (Mair and Hembrook 2008). To further prove the efficacy of ILN-DBS in an AD model, we first applied ILN-DBS to rats with intraventricular Aβ infusion. AD has been simulated and reproduced via both transgenic and non-transgenic animal models (Yamada and Nabeshima 2000). Intraventricular or intracerebral Aβ injection, in one of the non-transgenic animal models, has led to deficits in short-term memory, long-term memory, and object recognition in rats (O'hare et al. 1999; Nakamura et al. 2001). Changes in dendritic spine density and morphology (structural synaptic plasticity) are strongly associated with memory function (Bliss and Gardner-Medwin 1973; Guan et al. 2009). Dynamic changes of synaptic plasticity are proposed to be one of mechanistic for memory formation and storage. In fact, it has been repeatedly demonstrated that various internal and external factors could change spatial learning and dendritic spines (Chen et al. 2009a; b). The underpinnings of cognitive impairment caused by Aβ deposition in AD remain elusive. After 14 days of Aβ infusion, we showed that Aβ remarkably decreased the spine densities on

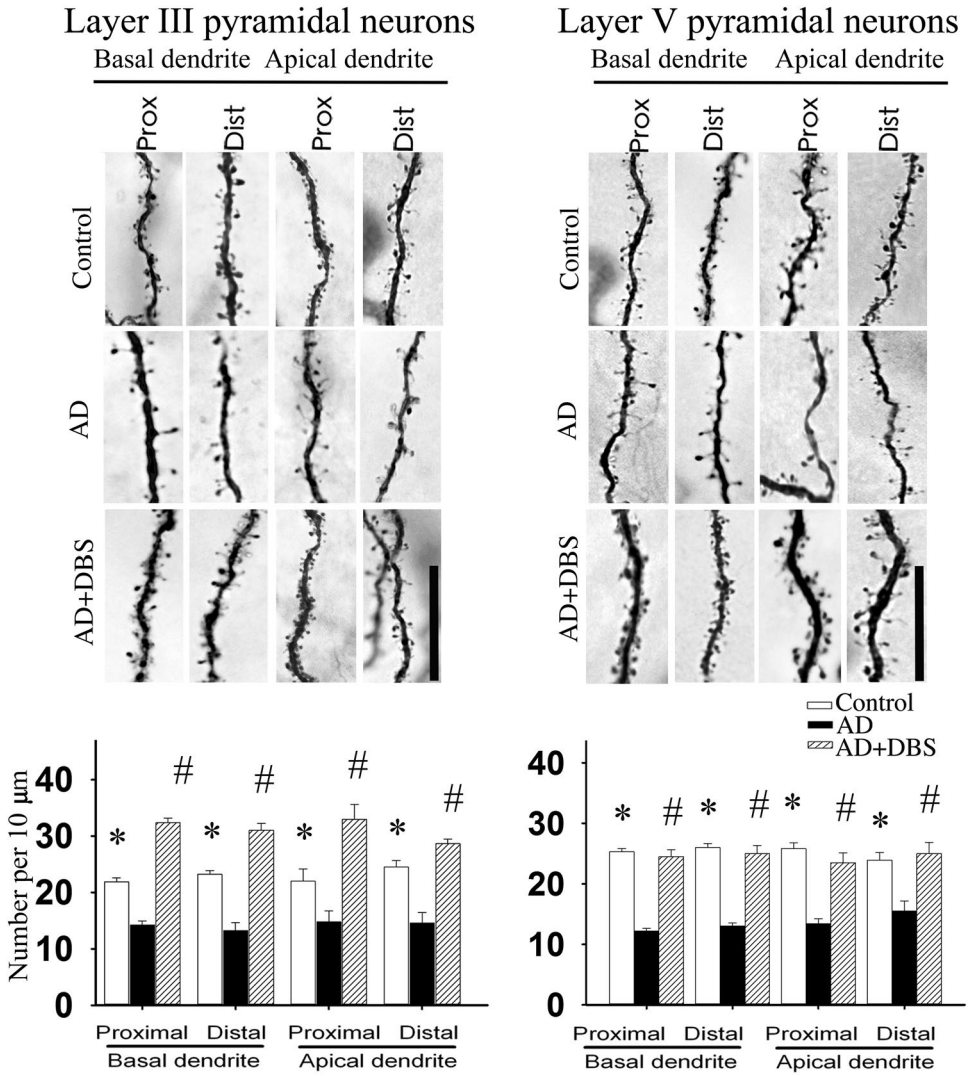

Fig. 6 ILN-DBS also reversed the Aβ-induced reduction in dendritic spine densities on mPFC pyramidal neurons. Upper panels: composite micrographs of representative basal and apical dendrite segments for mPFC Layer III pyramidal neurons (left column) and layer V pyramidal neurons (right column) from naïve control (upper row), AD (middle row), and AD + ILN-DBS (lower row) groups. Spine densities on the proximal and distal basal and apical dendrites for each group are shown below the corresponding columns. ILN-DBS reversed the Aβ-induced decrease in the density of dendritic spines over the entire dendritic arbor of mPFC layer III and layer V pyramidal neurons. $^{*}p < 0.05$, naïve control vs. AD; $^{\#}p < 0.05$, AD vs. AD + ILN-DBS. Scale bar = 10 µm. Error bars represent SEM

pyramidal neurons in both the hippocampus and the mPFC. This finding further highlights the ability of soluble Aβ to initiate synaptic dysfunction and structural changes that contribute to cognitive deficit (Spires-Jones et al. 2007; Spires-Jones and Knafo 2011). Furthermore, ILN-DBS restored the Aβ-induced decrease in dendritic spine density on pyramidal neurons. DBS has been shown to improve the electrophysiological synaptic plasticity of neurons (Sui et al. 2014). In addition, amelioration of the impairment of hippocampal synaptic plasticity caused by soluble Aβ oligomer has been demonstrated for external stimuli such as environmental novelty (Li et al. 2013). Taken together, our results suggest that rostral ILN-DBS can also potentiate memory repair through structural synaptic plasticity modulation. In recent years, the correlation between synaptic activity and Aβ pathogenesis in AD is debated. Synaptic activity dynamically regulates Aβ secretion, which is implicated as mechanistic of AD and its cognitive impairment (Tampellini et al. 2010). While some evidences showed that endogenous higher synaptic activity increases interstitial fluid Aβ level and subsequent Aβ plaque deposition, other data revealed that exogenous synaptic activation is beneficial on Aβ-related synaptic and behavioral impairment in AD (Tampellini et al. 2010; Bero et al. 2011). Our findings suggest that rostral ILN-DBS may synchronize synaptic activation and modulate Aβ levels and thereby spines.

Shirvalkar et al. used unilateral electrical stimulation of ILN in the thalamus in normal rats to enhance cognitive performance and achieve widespread cerebral, cortical and hippocampal neural activation (Shirvalkar et al. 2006). In addition to facilitating object recognition memory, ILN-DBS also increased exploratory motor behavior in normal rats, which is consistent with the increase in arousal status. The effect of ILN-DBS on memory enhancement in normal rats was confirmed in another study using memory-guided response (Mair and Hembrook 2008). Cognitive enhancement has been observed in several studies of diseased humans with obesity (Hamani et al. 2008) and epilepsy

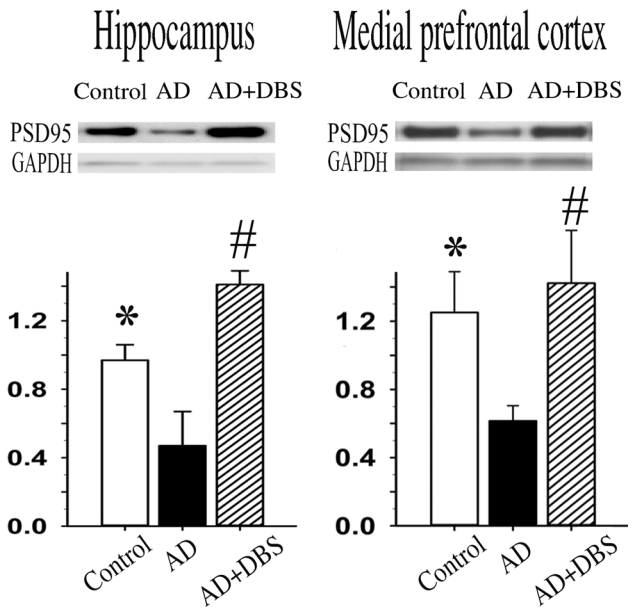

Fig. 7 ILN-DBS reversed Aβ-induced downregulation of PSD-95 (a marker of glutamatergic synapses) in mPFC and hippocampal CA as evidenced by western blotting. GAPDH was used as the gel loading control. $^{*}p < 0.05$, naïve control vs. AD; $^{\#}p < 0.05$, AD vs. AD + ILN-DBS

(Suthana et al. 2012) and normal mice (Stone et al. 2011); DBS of the fornix or entorhinal cortex rescued impaired memory. Collectively, these reports all indicate that administering DBS to a specific target area within a cognitive circuit of the brain could restore cognition through the repair of defective neural plasticity (Toda et al. 2008; Laxton et al. 2010). However, these beneficial effects of DBS on cognitive performance have not been explored in the setting of AD. Thus, our results further highlight the notion that rostral ILN-DBS could also be applied to rat models of AD to ameliorate the spatial memory learning deficit as well as the underlying impaired synaptic plasticity.

The levels of glutamate transmission and associated vesicular glutamate transporters play pivotal roles in the refinement of the dendritic structures of pyramidal neurons, as well as in synaptic plasticity and cognition (He et al. 2012). Subthalamic deep brain stimulation has been shown to achieve therapeutic effects in Parkinson's disease through modulation of glutamatergic terminals and transmission (Walker et al. 2012). Consistent with behavioral performance, our findings showed that soluble Aβ oligomers significantly decreased spine densities on pyramidal neurons of both the mPF and hippocampus, with parallel reductions of PSD-95. Both results suggest a dramatic reduction of glutamatergic excitatory synapses (Deng et al. 2014). PSD-95 anchors synaptic proteins and interacts with NMDA receptors to play important roles in the stabilization of synaptic changes during long-term potentiation and synaptic plasticity (Xu 2011; Meyer et al. 2014). Rostral ILN-DBS can increase the reduced dendritic spine densities, and the levels of PSD-95 further support that ILN-DBS may facilitate cognition and memory through modulation of glutamatergic transmission.

Rostral ILN-DBS was shown to increase neural activity in the cerebral cortex and arousal in rats and patients with cognitive impairment (Shirvalkar et al. 2006; Schiff et al. 2007). Based on the presumption that arousal status is closely related with memory acquisition and consolidation, we began our experiments and found that ILN-DBS did restore dysfunctional memory circuits and structural neural plasticity in rats with intraventricular Aβ infusion (Barondes and Cohen 1968; Saab et al. 2009; Mair et al. 2011). Whether these behavioral changes in our results could be attributed to increased arousal or modulation of thalamocortical circuits remains unknown (López-Bendito and Molnár 2003; Smith et al. 2009; Staudigl et al. 2012). A crucial issue for clinical applicability of ILN-DBS is whether the duration or timing of stimulation is optimal, an issue that should be addressed in future studies (Mair and Hembrook 2008; Suthana et al. 2012). Another limitation of our study is the lack of a comparison group receiving DBS but without Aβ infusion. Therefore, we cannot exclude stimulation-independent effects, such as reparative responses from electrode-induced tissue damage. However, the 'off' state appears to have little clinical efficacy in patients with DBS electrode implantation, indicating that improvements in AD-like pathology and spatial memory deficits were likely stimulus dependent. Further, our AD + sham group showed comparable decreased memory performance with AD group and DBS ameliorated this impairment. Previous studies also have reported that ILN-DBS stimulation settings similar to those used in this study improved cognition compared to sham stimulation (Shirvalkar et al. 2006; Tsai et al. 2016). One additional limitation is that we implanted an osmotic minipump at the contralateral hemisphere for intraventricular Aβ infusion and this created an obstacle for implantation of DBS electrode on this hemisphere. However, unilateral target deep brain stimulation has been shown to improve cognitive function and memory task performance (Shirvalkar et al. 2010).

Conclusion

DBS to the rat thalamic intralaminar nucleus at clinically relevant settings can restore impaired spatial memory and structural synaptic plasticity of glutamatergic synapses induced by Aβ infusion. Our findings support the potential of ILN-DBS for AD treatment.

Acknowledgments We are grateful to Professor Yu-Ru Kou and Dr. Ben S. Huang for discussion, comments, and English editing of the paper.

Authors' contributions 1. Research project: A. conception: ST, SC, SL, GT, B. execution: ST, GT; 2. statistical analysis: A. design and execution: ST, B. review and critique: SC, SL, GT; 3. manuscript preparation: A. writing of the first draft: ST, B. review and critique: SC, GT. All authors read and approved the final manuscript.

Funding Tzu Chi University: TCIRP 104001-0, 104001-05, 107001-01, and 107001-04; Ministry of Science and Technology of Taiwan: 104-2320-B-320-001-MY3; 107-2320-B-320-006 and 108-2314-B-303-014.

Compliance with ethical standards

Competing interests. The authors declare that they have no competing interest.

Ethics approval and consent to participate This animal study has ethical approval.

References

Ansari MA, Roberts KN, Scheff SW (2008) A time course of contusion-induced oxidative stress and synaptic proteins in cortex in a rat model of TBI. J Neurotrauma 25(5):513–526. https://doi.org/10.1089/neu.2007.0451

Barondes SH, Cohen HD (1968) Arousal and the conversion of "short-term" to "long-term" memory. Proc Natl Acad Sci USA 61:923–929

Bero AW, Yan P, Roh JH et al (2011) Neuronal activity regulates the regional vulnerability to amyloid-β deposition. Nat Neurosci 14(3):750–756. https://doi.org/10.1038/nn.2801

Bliss TV, Gardner-Medwin AR (2009) Design and development of a new facility for teaching and research in clinical anatomy. Anatomical Sciences Education 2:357–374

Chen J-R, Chen JR, Yan Y-T et al

Chen J-R, Wang T-J, Huang H-Y et al (2009b) Fatigue reversibly reduced cortical and hippocampal dendritic spines concurrent with compromise of motor endurance and spatial memory. Neuroscience 161:1104–1113. https://doi.org/10.1016/j.neuroscience.2009.04.022

Chen J-R, Wang T-J, Lim S-H et al (2013) Testosterone modulation of dendritic spines of somatosensory cortical pyramidal neurons. Brain Struct Funct 218:1407–1417. https://doi.org/10.1007/s00429-012-0465-7

Cholvin T, Loureiro M, Cassel R et al (2016) Dorsal hippocampus and medial prefrontal cortex each contribute to the retrieval of a recent spatial memory in rats. Brain Struct Funct 221:91–102. https://doi.org/10.1007/s00429-014-0894-6

Deng Y, Xiong Z, Chen P et al (2014) β-Amyloid impairs the regulation of N-methyl-D-aspartate receptors by glycogen synthase kinase 3. Neurobiol Aging 35:449–459. https://doi.org/10.1016/j.neurobiolaging.2013.08.031

Furuyashiki T, Fujisawa K, Fujita A, Madaule P, Uchino S, Mishina M, Bito H, Narumiya S (1999) Citron, a Rho-target, interacts with PSD-95/SAP-90 at glutamatergic synapses in the thalamus. J Neurosci 19(1):109–118

Gold JJ, Squire LR (2006) The anatomy of amnesia: neurohistological analysis of three new cases. Learn Mem 13:699–710. https://doi.org/10.1101/lm.357406

Guan J-S, Haggarty SJ, Giacometti E et al (2009) HDAC2 negatively regulates memory formation and synaptic plasticity. Nature 459:55–60. https://doi.org/10.1038/nature07925

Hamani C, McAndrews MP, Cohn M et al (2008) Memory enhancement induced by hypothalamic/fornix deep brain stimulation. Ann Neurol 63:119–123. https://doi.org/10.1002/ana.21295

Hamani C, Stone SS, Garten A et al (2011) Memory rescue and enhanced neurogenesis following electrical stimulation of the anterior thalamus in rats treated with corticosterone. Exp Neurol 232:100–104. https://doi.org/10.1016/j.expneurol.2011.08.023

He H, Mahnke AH, Doyle S et al (2012) Neurodevelopmental role for VGLUT2 in pyramidal neuron plasticity, dendritic refinement, and in spatial learning. J Neurosci 32:15886–15901. https://doi.org/10.1523/JNEUROSCI.4505-11.2012

Herrington TM, Cheng JJ, Eskandar EN (2016) Mechanisms of deep brain stimulation. J Neurophysiol 115:19–38. https://doi.org/10.1152/jn.00281.2015

Hescham S, Lim LW, Jahanshahi A et al (2013a) Deep brain stimulation of the forniceal area enhances memory functions in experimental dementia: the role of stimulation parameters. Brain Stimul 6:72–77. https://doi.org/10.1016/j.brs.2012.01.008

Hescham S, Lim LW, Jahanshahi A et al (2013b) Deep brain stimulation of the forniceal area enhances memory functions in experimental dementia: The role of stimulation parameters. Brain Stimul 6:72–77. https://doi.org/10.1016/j.brs.2012.01.008

Hescham S, Jahanshahi A, Schweimer JV et al (2016) Fornix deep brain stimulation enhances acetylcholine levels in the hippocampus. Brain Struct Funct 221:4281–4286. https://doi.org/10.1007/s00429-015-1144-2

Hescham S, Temel Y, Schipper S et al (2017) Fornix deep brain stimulation induced long-term spatial memory independent of hippocampal neurogenesis. Brain Struct Funct 222:1069–1075. https://doi.org/10.1007/s00429-016-1188-y

Laxton AW, Tang-Wai DF, McAndrews MP et al (2010) A phase I trial of deep brain stimulation of memory circuits in Alzheimer's disease. Ann Neurol 68:521–534. https://doi.org/10.1002/ana.22089

Leoutsakos JS, Yan H, Anderson WS, Asaad WF, Baltuch G, Burke A, Chakravarty MM, Drake KE, Foote KD, Fosdick L, Giacobbe P, Mari Z, McAndrews MP, Munro CA, Oh ES, Okun MS, Pendergrass JC, Ponce FA, Rosenberg PB, Sabbagh MN, Salloway S, Tang-Wai DF, Targum SD, Wolk D, Lozano AM, Smith GS, Lyketsos CG (2018) Deep brain stimulation targeting the fornix for mild alzheimer dementia (the ADvance Trial): a two year follow-up including results of delayed activation. J Alzheimer's Dis 64(2):597–606. https://doi.org/10.3233/JAD-180121

Leplus A, Lauritzen I, Melon C et al (2019) Chronic fornix deep brain stimulation in a transgenic Alzheimer's rat model reduces amyloid burden, inflammation, and neuronal loss. Brain Struct Funct 224:363–372. https://doi.org/10.1007/s00429-018-1779-x

Li S, Jin M, Zhang D et al (2013) Environmental novelty activates β2-adrenergic signaling to prevent the impairment of hippocampal LTP by Aβ oligomers. Neuron 77:929–941. https://doi.org/10.1016/j.neuron.2012.12.040

López-Bendito G, Molnár Z (2003) Thalamocortical development: how are we going to get there? Nat Rev Neurosci 4:276–289. https://doi.org/10.1038/nrn1075

Luebke JI, Weaver CM, Rocher AB et al (2010) Dendritic vulnerability in neurodegenerative disease: insights from analyses of cortical pyramidal neurons in transgenic mouse models. Brain Struct Funct 214:181–199. https://doi.org/10.1007/s00429-010-0244-2

Mair RG, Hembrook JR (2008) Memory enhancement with event-related stimulation of the rostral intralaminar thalamic nuclei.

J Neurosci 28:14293–14300. https://doi.org/10.1523/JNEUROSCI.3301-08.2008
Mair RG, Onos KD, Hembrook JR (2011) Cognitive activation by central thalamic stimulation: the Yerkes–Dodson law revisited. Dose Response 9:313–331. https://doi.org/10.2203/dose-response.10-017.Mair
Malm T, Ort M, Tähtivaara L et al (2006) beta-Amyloid infusion results in delayed and age-dependent learning deficits without role of inflammation or beta-amyloid deposits. Proc Natl Acad Sci USA 103:8852–8857. https://doi.org/10.1073/pnas.0602896103
Meyer D, Bonhoeffer T, Scheuss V (2014) Balance and stability of synaptic structures during synaptic plasticity. Neuron 82(2):430–543. https://doi.org/10.1016/j.neuron.2014.02.031
Nakamura S, Nakamura S, Murayama N et al (2001) Progressive brain dysfunction following intracerebroventricular infusion of beta1–42-amyloid peptide. Brain Res 912:128–136. https://doi.org/10.1016/S0006-8993(01)02704-4
Nitta A, Nitta A, Itoh A et al (1994) β-Amyloid protein-induced Alzheimer's disease animal model. Neurosci Lett 170:63–66. https://doi.org/10.1016/0304-3940(94)90239-9
O'hare E, Weldon DT, Mantyh PW et al (1999) Delayed behavioral effects following intrahippocampal injection of aggregated Aβ(1–42). Brain Res 815:1–10. https://doi.org/10.1016/S0006-8993(98)01002-6
Ovsepian SV, O'Leary VB, Záborszky L (2016) Cholinergic mechanisms in the cerebral cortex: beyond synaptic transmission. Neuroscientist 22:238–251. https://doi.org/10.1177/1073858415588264
Saab BJ, Georgiou J, Nath A et al (2009) NCS-1 in the dentate gyrus promotes exploration, synaptic plasticity, and rapid acquisition of spatial memory. Neuron 63:643–656. https://doi.org/10.1016/j.neuron.2009.08.014
Saalmann YB (2014) Intralaminar and medial thalamic influence on cortical synchrony, information transmission and cognition. Front Syst Neurosci 8:83. https://doi.org/10.3389/fnsys.2014.00083
Scarpini E, Scheltens P, Feldman H (2003) Treatment of Alzheimer's disease: current status and new perspectives. The Lancet Neurology 2:539–547
Schiff ND, Giacino JT, Kalmar K et al (2007) Behavioural improvements with thalamic stimulation after severe traumatic brain injury. Nature 448:600–603. https://doi.org/10.1038/nature06041
Schubert D, Kötter R, Staiger JF (2007) Mapping functional connectivity in barrel-related columns reveals layer- and cell type-specific microcircuits. Brain Struct Funct 212:107–119. https://doi.org/10.1007/s00429-007-0147-z
Shirvalkar P, Seth M, Schiff ND, Herrera DG (2006) Cognitive enhancement with central thalamic electrical stimulation. Proc Natl Acad Sci USA 103:17007–17012. https://doi.org/10.1073/pnas.0604811103
Shirvalkar PR, Rapp PR, Shapiro ML (2010) Bidirectional changes to hippocampal theta-gamma comodulation predict memory for recent spatial episodes. Proc Natl Acad Sci USA 107:7054–7059. https://doi.org/10.1073/pnas.0911184107
Smith AC, Shah SA, Hudson AE et al (2009) A Bayesian statistical analysis of behavioral facilitation associated with deep brain stimulation. J Neurosci Methods 183:267–276. https://doi.org/10.1016/j.jneumeth.2009.06.028
Spires-Jones T, Knafo S (2011) Spines, plasticity, and cognition in Alzheimer's model mice. Neural Plasticity
Spires-Jones TL, Meyer-Luehmann M, Osetek JD et al (2007) Impaired spine stability underlies plaque-related spine loss in an Alzheimer's disease mouse model. Am J Pathol 171:1304–1311. https://doi.org/10.2353/ajpath.2007.070055
Srivareerat M, Tran TT, Alzoubi KH, Alkadhi KA (2009) chronic psychosocial stress exacerbates impairment of cognition and long-term potentiation in—amyloidrat model of Alzheimer's disease. BPS 65:918–926. https://doi.org/10.1016/j.biopsych.2008.08.021
Staudigl T, Zaehle T, Voges J et al (2012) Memory signals from the thalamus: early thalamocortical phase synchronization entrains gamma oscillations during long-term memory retrieval. Neuropsychologia 50:3519–3527. https://doi.org/10.1016/j.neuropsychologia.2012.08.023
Stone SSD, Teixeira CM, Devito LM et al (2011) Stimulation of entorhinal cortex promotes adult neurogenesis and facilitates spatial memory. J Neurosci 31:13469–13484. https://doi.org/10.1523/JNEUROSCI.3100-11.2011
Sui L, Huang S, Peng B et al (2014) Deep brain stimulation of the amygdala alleviates fear conditioning-induced alterations in synaptic plasticity in the cortical–amygdala pathway and fear memory. J Neural Transm 121:773–782. https://doi.org/10.1007/s00702-014-1183-5
Suthana N, Haneef Z, Stern J et al (2012) Memory enhancement and deep-brain stimulation of the entorhinal area. N Engl J Med 366:502–510. https://doi.org/10.1056/NEJMoa1107212
Tampellini D, Capetillo-Zarate E, Dumont M et al (2010) Effects of synaptic modulation on beta-amyloid, synaptophysin, and memory performance in Alzheimer's disease transgenic mice. J Neurosci 30:14299–14304. https://doi.org/10.1523/JNEUROSCI.3383-10.2010
Toda H, Hamani C, Fawcett AP et al (2008) The regulation of adult rodent hippocampal neurogenesis by deep brain stimulation. J Neurosurg 108:132–138. https://doi.org/10.3171/JNS/2008/108/01/0132
Tsai S-T, Chen L-J, Wang Y-J et al (2016) Rostral intralaminar thalamic deep brain stimulation triggered cortical and hippocampal structural plasticity and enhanced spatial memory. Stereotact Funct Neurosurg 94:108–117. https://doi.org/10.1159/000444759
Van der Werf YD, Witter MP, Groenewegen HJ (2002) The intralaminar and midline nuclei of the thalamus. Anatomical and functional evidence for participation in processes of arousal and awareness. Brain Res Brain Res Rev 39:107–140
Vorhees CV, Williams MT (2006) Morris water maze: procedures for assessing spatial and related forms of learning and memory. Nat Protoc 1:848–858. https://doi.org/10.1038/nprot.2006.116
Walker RH, Moore C, Davies G et al (2012) Effects of subthalamic nucleus lesions and stimulation upon corticostriatal afferents in the 6-hydroxydopamine-lesioned rat. PLoS ONE 7:e32919. https://doi.org/10.1371/journal.pone.0032919
Xu W (2011) PSD-95-like membrane associated guanylate kinases (PSD-MAGUKs) and synaptic plasticity. Curr Opin Neurobiol 21:306–312. https://doi.org/10.1016/j.conb.2011.03.001
Yamada K, Nabeshima T (2000) Animal models of Alzheimer's disease and evaluation of anti-dementia drugs. Pharmacol Ther 88:93–113. https://doi.org/10.1016/S0163-7258(00)00081-4
Záborszky L, Gombkoto P, Varsanyi P et al (2018) Specific basal forebrain–cortical cholinergic circuits coordinate cognitive operations. J Neurosci 38:9446–9458. https://doi.org/10.1523/JNEUROSCI.1676-18.2018

Publisher's Note Springer Nature remains neutral with regard to jurisdictional claims in published maps and institutional affiliations.